

**UCLA**

**UCLA Previously Published Works**

**Title**

Digital Microfluidics: A New Paradigm for Radiochemistry

**Permalink**

<https://escholarship.org/uc/item/3kk0x3wv>

**Journal**

Molecular Imaging, 14(12)

**ISSN**

1535-3508

**Authors**

Keng, Pei Yuin  
van Dam, R Michael

**Publication Date**

2015-12-01

**DOI**

10.2310/7290.2015.00030

Peer reviewed



# HHS Public Access

Author manuscript

*Mol Imaging*. Author manuscript; available in PMC 2016 February 01.

Published in final edited form as:

*Mol Imaging*. 2015 December 5; 14: 13–14. doi:10.2310/7290.2015.00030.

## Digital microfluidics – a new paradigm for radiochemistry

Pei Yuin Keng and R. Michael van Dam\*

Crump Institute for Molecular Imaging and Department of Molecular & Medical Pharmacology  
University of California, Los Angeles

### Abstract

The emerging technology of digital microfluidics is opening up the possibility to perform radiochemistry at the microliter scale to produce tracers for positron emission tomography (PET) labeled with fluorine-18 or other isotopes. Working at this volume scale not only reduces reagent costs, but also improves specific activity (SA) by reduction of contamination by the stable isotope. This technology could provide a practical means to routinely prepare high SA tracers for applications such as neuroimaging, and could make it possible to routinely achieve high SA using synthesis strategies such as isotopic exchange. Reagent droplets are controlled electronically, providing high reliability, a compact control system, and flexibility for diverse syntheses with a single chip design. The compact size may enable the development of a self-shielded synthesizer that does not require a hot cell. This article reviews the progress of this technology and its application to the synthesis of PET tracers.

### Keywords

novel chemistry methods and approaches; advances in PET/SPECT probes; lab-on-a-chip devices; radiochemistry; PET

### Introduction

The unique capabilities of positron emission tomography (PET) to provide extremely sensitive, whole-body images of specific biochemical processes or biomolecular targets *in vivo* are providing increasing value in research, drug development, and patient care. Currently, most PET studies involve imaging glucose metabolism after injection with the tracer 2-[<sup>18</sup>F]fluoro-2-deoxy-D-glucose ([<sup>18</sup>F]FDG), enabling, for example, the diagnosis and staging of cancer, monitoring response to therapy, evaluating cardiac function, and distinguishing certain neurological disorders [1]. In combination with other tracers, PET can provide even more specific diagnoses based on the detection of underlying molecular alterations associated with many health conditions [2, 3]. PET also provides tremendous benefit in the process of developing new targeted drugs and companion diagnostics for precision medicine [4], as well as in the development of novel gene- and cell-based therapies

---

Corresponding author: R. Michael van Dam, Associate Professor, Crump Institute for Molecular Imaging, UCLA Department of Molecular & Medical Pharmacology, Room 4323, California Nanosystems Institute, 570 Westwood Plaza, Building 114, Mail Code 722710, Los Angeles, CA 90095, mvandam@mednet.ucla.edu, Phone: 310-206-6507, FAX: 310-206-8975.

[5]. Routine access to tracers other than [ $^{18}\text{F}$ ]FDG could accelerate progress in all of these areas.

Because tracers are radioactive, their preparation requires specialized (and expensive) equipment to protect the radiochemist who prepares them, and the short lifetimes of the positron-emitting isotopes (i.e., 110 min for fluorine-18) require that the infrastructure, technology and expert personnel for their production be replicated and distributed across many facilities to supply different geographical areas. Currently, commercial production of PET tracers such as [ $^{18}\text{F}$ ]FDG occurs in a "satellite" manner. Radiopharmacies manufacture large batches that can be subdivided into many unit doses and then distributed to patients within a local area to leverage economies of scale and offer the compounds at an affordable price. However, this method of reducing price does not scale to greater numbers of different tracers. As the diversity of PET tracers increases in medical care and research, the demand for each particular tracer likely decreases, and it becomes more challenging to coordinate needs for tracers among imaging centers. Each radiopharmacy would need to produce a greater number of batches (i.e., of different tracers), and each batch would be subdivided into a smaller number of doses, increasing the cost for each patient.

To increase the diversity of tracers available at low cost will require a fundamental reduction in the production cost, and this requires innovative new technologies. Several trends in radiosynthesizers have emerged toward this end [6]. For example, kit-based synthesizers can be configured to make different probes on the same or subsequent days merely by installing different disposable "cassettes", reducing the need for a dedicated, custom-configured synthesizer for every probe. Another trend is miniaturized radiosynthesizers, which have the potential to dramatically reduce the cost of the synthesizer itself, as well as the amount of shielding infrastructure needed for operation. If small enough, the synthesizer can potentially be self-shielded, eliminating the need for hot cells and associated infrastructure. Other emerging technologies such as automated quality control testing [7] can further reduce equipment, personnel, and documentation costs and simplify production.

A key technology driving miniaturization is the use of microfluidics. It has been well-established that the geometry of microfluidic devices offers many advantages for the synthesis of short-lived radiopharmaceuticals [8–14]. In particular, the small dimensions enable improved control of reaction conditions via rapid mixing and efficient heat transfer, leading in some cases to faster reactions and improved selectivity, and thus higher yields. An additional advantage is suppression of the effects of radiolysis because a large fraction of the positron energy is absorbed by the walls of the microfluidic rather than the tracer solution [15].

Since the inception of using microfluidics for the synthesis of PET radiotracers in 2002 [16], most reports have described "flow-through" microreactors, where reactions occur by flowing reagent streams through mixers and pre-heated capillary tubes, microchannels, or other structures [17–23]. A wide range of tracers has been demonstrated using this approach [14], in many cases exhibiting extremely short residence times (i.e. time spent by the reagents in the heated region of the reactor) or significant reductions in precursor concentrations compared to the macroscale. Flow-through production of a tracer for use in

humans has been reported recently [24]. However, despite small reactor dimensions, the overall synthesizers based on flow-through microfluidics are comparable in size to macroscale systems. One limitation preventing further miniaturization is that some of the radiosynthesis steps such as solvent exchange (evaporation of solvent, and reconstitution of residue in the next solvent) must be performed using conventional apparatus. Operating volumes for production runs on flow-through systems are generally comparable to macroscale systems (i.e., 100s of microliters to several milliliters).

A different class of microfluidic device based on batch reactions with small total volumes (i.e., microliter) offers the geometrical advantages described above plus additional advantages, including reduced consumption of expensive reagents (e.g. precursors or proteins), integration of all synthesis steps on a single chip, simpler purification processes (due to greatly reduced quantities of reagents), higher radioisotope concentration (which improves reaction kinetics and is helpful in reducing amount of carrier in carrier-added syntheses) and higher specific activity (SA) due to a reduction in contamination with the non-radioactive isotope from reagents and wetted materials. By using an auxiliary miniature ion-exchange cartridge, large amounts of radioactivity, comparable to what can be used in macroscale systems (e.g., 1 Ci), can be concentrated into volumes compatible with these chips.

Batch microsynthesis devices for multistep radiochemistry were first implemented in silicone rubber (poly(dimethylsiloxane), PDMS) in 2005 in a proof-of-concept device with 40 nL reaction volume [25] and were later scaled up to a 5  $\mu$ L reaction capable of production of mCi amounts of  $^{18}\text{F}$ -labeled tracers [26]. Unfortunately, due to suspected reaction between PDMS and  $^{18}\text{F}$ fluoride under certain conditions [27], radioactivity losses were high and device reliability was low. For certain reactions under mild conditions (e.g. labeling with radiometals [20] or  $^{18}\text{F}$ -labeled prosthetic groups [28]), PDMS continues to be used. For applications involving harsh chemistry, switching to more inert materials was necessary to eliminate losses and improve the reliability. Using a chip with a 50  $\mu$ L capacity reactor made of glass and polydicyclopentadiene plastic, the synthesis of several tracers has been shown, including the demonstration of production for human imaging [29, 30], establishing the relevance of the micro-batch format.

More recently, we demonstrated, in collaboration with Chang-Jin Kim (Dept. of Mechanical and Aerospace Engineering, UCLA), the successful radiosynthesis of several  $^{18}\text{F}$ -labeled compounds using another type of batch microfluidic device with variable volume (1–17  $\mu$ L) based on the digital manipulation of droplets between two parallel plates [31–33]. Control of droplets in these electrowetting-on-dielectric (EWOD) microchips is entirely electronic [34], which provides inherent reliability by eliminating the need for moving parts, and eliminates the need for bulky valve actuators within the radiation shielding. These EWOD microchips are constructed from chemically-inert and thermally-stable materials (glass, indium tin oxide, gold, silicon nitride, and Teflon AF), offering excellent reagent compatibility (include with  $^{18}\text{F}$ fluoride), and thus wide flexibility in terms of reagents, reaction conditions, and therefore tracers. In collaboration with Sofie Biosciences, Inc., significant progress has been made toward automation and interfacing to enable safe and routine use of these chips. These efforts will enable exploration of microliter-scale synthesis of additional

tracers on EWOD chips in clinically-relevant amounts. Very recently, another type of droplet approach was reported in which 50–60  $\mu\text{L}$  aqueous reagent droplets (containing magnetic beads) were manipulated on top of a Teflon sheet, via a magnet mounted on a robotic arm, to synthesize sulfonyl [ $^{18}\text{F}$ ]fluoride [35]. It appears this platform could provide similar advantages to EWOD microfluidics, though the droplet manipulation scheme may be more limited and require a bulkier actuating mechanism.

In this review, we present the progress made in EWOD digital microfluidic technology for radiosynthesis, and outline remaining challenges to bring it into mainstream use in the field of radiochemistry, and ultimately onto the benchtop and into the clinic.

## Digital chemistry on chip

The EWOD microchip (Figure 1) contains two-dimensional (2D) pattern of electrodes that manipulates droplets through locally-applied electric fields [36]. For many types of liquid, an electric field can change the interaction between a droplet and the surface via the phenomenon of “electrowetting”. As electrical potential is applied to an electrode, the contact angle between the droplet and the electrode surface is reduced, thus creating a more wetting surface. Applying the potential adjacent to a droplet causes the droplet to move toward the wetted electrode. By applying a time-varying (AC) electric field, the phenomenon of dielectrophoresis can also be leveraged to create forces on droplets. A typical EWOD chip is composed of two parallel substrates, a bottom plate containing individually-addressed actuation electrodes, and a cover plate serving as the ground electrode, with droplets sandwiched in between [37]. Both substrates are layered with a conductor such as indium tin oxide (ITO), a dielectric layer, and a hydrophobic layer (e.g. Cytop or Teflon), though the dielectric layer is sometimes omitted on the cover plate. The hydrophobic layer prevents the droplet from sticking to the surface and enhances the response to electrical actuation, enabling many droplet-medium combinations to be manipulated e.g.: water in oil [38], water in air [37], solvent or oil in air [39, 40], gas in water [41], etc. Solid materials (e.g. solid catalysts or magnetic beads) can also be manipulated in the form of suspensions [42]. Though EWOD devices can also be operated in an “open” configuration provided ground wires or coplanar electrodes are included to ground the electric field, many droplet-medium combinations cannot be effectively manipulated and therefore the closed configuration is preferred.

By locally applying appropriate voltage sequences, numerous unit operations can be performed (Figure 1) such as dispensing, moving, and mixing of reagent droplets [34]. On-chip electrodes can also be used for resistive heating and temperature sensing to achieve precise temperature control to facilitate chemical reactions or evaporation steps (e.g. for solvent exchange). Compared to other types of microfluidic devices, the open sides of the EWOD chip are advantageous for removal of solvent vapor, though measures must be taken to avoid the problem of unwanted evaporation during reaction steps.

## Digital radiochemistry on chip

### Synthesis of [<sup>18</sup>F]FDG

Combining the above unit operations, the multistep synthesis of [<sup>18</sup>F]FDG was successfully demonstrated on an EWOD chip [31] (see Figure 2). The synthesis began with loading and drying of droplets of [<sup>18</sup>F]fluoride complexed with a phase-transfer catalyst, followed by loading of droplets of acetonitrile (MeCN) and azeotropic distillation. Next, the precursor, mannose triflate, in 4  $\mu$ L of dimethyl sulfoxide (DMSO) was added, followed by 12  $\mu$ L of MeCN to ensure filling of the whole heater region to dissolve the dried fluoride complex. Upon heating, this MeCN rapidly evaporates, leaving primarily the DMSO for the duration of the fluorination reaction. Hydrolysis to remove the protecting groups and form [<sup>18</sup>F]FDG was performed by directly adding a mixture of hydrochloric acid and MeCN and then heating. The presence of residual DMSO from fluorination ( $\sim$ 0.2  $\mu$ L) did not impede this reaction, nor did it generate toxic byproducts under the harsh, acidic conditions.

It should be noted that to limit evaporation during the fluorination step, it was important to use a high boiling point solvent: in this case, DMSO (bp=189°C). DMSO is a versatile solvent for various types of chemical reactions, but it tends to be avoided in radiochemistry due to the difficulty in rapidly removing the solvent volume (typically 500–1000  $\mu$ L) after the reaction. However, due to the small volume used on EWOD chips compared to the macroscale, the use of DMSO is practical in microscale synthesis.

Furthermore, the volume is sufficiently small that simple dilution at the end of synthesis is sufficient to reduce the DMSO concentration below regulatory limits.

Despite a high fluorination efficiency and quantitative hydrolysis, the initially-reported synthesis exhibited a decay-corrected crude radiochemical yield (crude RCY) of 32 $\pm$ 15% (n=11), defined as the radioactivity of the crude reaction mixture multiplied by product purity (determined by radio-TLC) divided by the starting radioactivity. After extraction of the crude [<sup>18</sup>F]FDG product from the chip and purification using a custom-made cartridge, the decay-corrected radiochemical yield (RCY) was 22 $\pm$ 8% (n=11) [31], defined as the radioactivity of the isolated, purified product divided by the starting radioactivity. The final formulated product passed all quality control tests required for human use. Tests passed by wide margins due to the small amounts of reagents used in the synthesis. The purified [<sup>18</sup>F]FDG has been administered into both healthy and immune-compromised mice for preclinical PET imaging and no adverse effects on the health of the mice were observed [31].

Using a novel analytical tool for microfluidics chips based on imaging of Cerenkov radiation (arising from high-energy positrons traveling through the solvent and chip material) [43, 44], it was possible to account for the amount and distribution of radioactivity at multiple time points during the on-chip synthesis. After identification of steps with the highest losses, subsequent optimization and changes to the EWOD chip design led to an improved crude RCY of 72% [44]. Using simplified chips (with no electrical actuation), Koag *et al.* later studied the reaction kinetics and effect of cosolvent, and achieved an (isolated) RCY of 71.2% (n=5; standard deviation not reported) by using a bulky alcohol co-solvent during the

fluorination [45]. The overall synthesis time was not reported, but the fluorination reaction was shortened from 10 min to 3 min, and the hydrolysis step was shortened from 10 min to 2 min. These optimized results are comparable to conventional approaches for synthesis of [ $^{18}\text{F}$ ]FDG (see Table 1).

### Synthesis of other $^{18}\text{F}$ -labeled tracers

The same principles by which [ $^{18}\text{F}$ ]FDG was synthesized on the EWOD chip have been extended to many other tracers with one-pot synthesis protocols. Microscale synthesis processes with high and reproducible yield have been developed for several additional example compounds, including [ $^{18}\text{F}$ ]FLT [46, 47], [ $^{18}\text{F}$ ]fallypride [48] and [ $^{18}\text{F}$ ]SFB [33]. Table 1 summarizes these results. For all tracers except [ $^{18}\text{F}$ ]SFB, the microscale syntheses exhibited similar yields to the best reported in the literature using conventional or microscale synthesizers. The microscale synthesis times were somewhat longer; however, as discussed later, these times are expected to improve with increased automation. It should be appreciated that Table 1 is comparing the results from a technology in development (EWOD) with results from commercial technologies that are currently being used for clinical applications.

In general, the microscale syntheses followed the same reaction pathways as their macroscale counterparts, but sometimes required significant changes in the particular conditions (e.g., solvents or concentrations). Table 2 summarizes the results of a systematic exploration in our group of the impact on fluorination efficiency of several reaction conditions. During the optimization process, an understanding of several general rules of microdroplet radiochemistry was gleaned that could be used to help translate a known macroscale protocol onto the EWOD chip.

In particular, reagent concentration typically needs to be increased in the chip to obtain high and reliable yield. For example, the fluorination efficiency of the [ $^{18}\text{F}$ ]FLT precursor on chip increased from 51% to 79% by doubling the reagent concentration from 45 to 90 mM. In the synthesis of [ $^{18}\text{F}$ ]FDG, [ $^{18}\text{F}$ ]FLT, [ $^{18}\text{F}$ ]fallypride and [ $^{18}\text{F}$ ]SFB, the highest yields were obtained using a precursor concentrations that were 5X, 2X, 5X, and 4X higher than the macroscale conditions, respectively. Other optimization studies conducted by Koag *et al.* on Teflon-coated glass substrates confirm this trend [45, 47]. Despite the higher concentrations, because the reaction volume is ~100–1000x lower than the macroscale, there is still a tremendous net reduction in the total amount of precursor consumed. Though flow-through microfluidic approaches have in some cases been shown to significantly lower the needed concentration of precursor compared to the macroscale, the overall consumption of precursor in EWOD is generally still lower than these approaches due to the difference in operating volumes.

An additional observed trend was that reduced droplet volume generally improved the reaction outcome. For example, the fluorination efficiency in microscale [ $^{18}\text{F}$ ]FLT synthesis improved from 79% to 94% when the reaction droplet volume was reduced from 4 to 2  $\mu\text{L}$  [46]. However, one must ensure there is sufficient volume that the reaction mixture is completely solvated for the entire length of reaction. If not, the reaction mixture dries out and low and unreliable fluorination efficiency was observed. In addition to improving



reaction yield, small volumes also help to accelerate solvent evaporation processes that are needed between steps in multistep synthesis protocols. This concept was especially helpful in reactions that evolve volatile intermediates, where longer duration of heating and evaporation steps is correlated with increased loss of radioactivity from the droplet. In the 3-step radiosynthesis of [ $^{18}\text{F}$ ]SFB, for example, the original conditions required 43 min of combined heating time for all reactions, while the reduced volume conditions avoided the need for a long DMSO evaporation step prior to hydrolysis and only required 9.5 min of combined heating time [49]. The shorter time reduced the loss of volatile species in this case, increasing the crude RCY of [ $^{18}\text{F}$ ]SFB from 32% to 50%.

### Increase in specific activity due to small volumes

For many of the tracers produced on the EWOD chip, the specific activity (SA) was observed to be significantly higher than typical macroscale reports. SA is defined as the amount of radioactivity per unit mass of a compound [50] and is related to the ratio of the radioactive (e.g. fluorine-18) to the non-radioactive (e.g. fluorine-19) versions of the isotope that get incorporated into the tracer. [ $^{19}\text{F}$ ]fluoride contamination originates from the [ $^{18}\text{O}$ ]water target, from materials in contact with the [ $^{18}\text{F}$ ]fluoride solution during cyclotron bombardment, delivery, and synthesis, as well as from reagents added before and during the radiofluorination reaction [51]. PET tracers with high specific activity are desirable, especially when imaging low-abundance receptors *in vivo* or for tracers that are radiolabeled version of pharmaceutically-active compounds. The need for high SA is heightened in the imaging of small animals [52]. An in-depth investigation to understand factors affecting SA led to the observation that the dependence of SA on reaction parameters was very different for macroscale (100–5000  $\mu\text{L}$ ) and microscale (2–8  $\mu\text{L}$ ) syntheses (Figure 3). At the macroscale, the specific activity strongly varied with the reaction volume (amount of reagents) as well as the starting activity, whereas in the microscale, the specific activity was much higher, and nearly constant ( $\sim 20 \text{ Ci}/\mu\text{mol}$ ), under all conditions. These results suggest that in the macroscale synthesis, contamination of reagents and solvents is the dominant source of fluorine-19, while at the microscale, these sources are negligible and the fluorine-19 from the cyclotron dominates [53].

Reduced volume also improves the specific activity or “effective specific activity” in cases where the precursor cannot be separated from the product (e.g., isotopic exchange reactions, or radiolabeling of proteins). If concentrations are kept similar to the macroscale, the microscale volume leads to a significant reduction in the amount of precursor, and therefore the amount of unreacted precursor present in the final product.

In addition to the need for very high SA in some imaging applications, the ability to achieve high SA can also have practical benefits such as extending the time that the SA of the batch of tracer is above some threshold value, enabling transport over larger distances or usage over longer periods of time.

Because high SA tracers can be produced in the chip even starting with low radioactivity (10s of mCi), the usual practice of starting with very high (Ci-level) amounts of radioactivity to achieve high SA can be avoided. This could greatly improve the safety of producing high specific activity tracers, and could increase their availability by not restricting their



production to laboratories that have cyclotrons and radiation safety infrastructure that is compatible with those high amounts.

## Automation and system integration

### Overview

In proof-of-concept radiosynthesis experiments [31, 33], reagents were delivered manually to tiny electrodes at the edge of the chip via pipette, and the crude product was collected using a pipette after manually separating the plates of the EWOD chip. In the following sections, progress toward automated operation of the EWOD chip and integration with all steps of the radiosynthesis process, from concentration of the radioisotope to purification, is reviewed. These advances increase safety and ease of use and dramatically reduce the synthesis time.

### Reagent Dispensing

A variety of approaches have been developed for automated loading of liquid reagents on demand to EWOD chips (reviewed in [54]). A common approach in other applications is the on-demand creation of droplets from large droplet “reservoirs” pre-loaded in the EWOD chip, but this approach is not suitable for storing liquids that are volatile or sensitive to air or moisture. A better approach is to store such reagents in sealed reservoirs such as glass vials until needed during the synthesis. Chemical manufacturers already package reagents and precursors in this format and there is considerable knowledge about the long-term shelf life of sensitive reagents.

One simple approach for controlled loading of reagents into EWOD chips used an electronically-controlled syringe pump to precisely meter the desired volume of reagent (Figure 4) [55]. Droplets were dispensed from a small blunt needle and could be pulled into the space between the plates by activating electrodes. Using this approach, accurate volumes of acetonitrile were successfully delivered multiple times during a radiosynthesis process to produce [ $^{18}\text{F}$ ]FDG [55].

Though successful in delivering precise volumes, a drawback of syringe pumps is that the wetted portions (i.e. syringe and valve) are difficult to clean between uses. In addition, a separate syringe pump and valve would be required for each reagent, adding to the size and complexity of the overall system. To address these issues, an alternative system was developed [56], in which inert gas pressure was applied to push the reagent up through a needle toward an inlet hole drilled in the chip (Figure 5). For aqueous reagents, the high contact angle ( $>90^\circ$ ) on the hydrophobic surface of the chip prevents spontaneous entry into the chip, allowing a small volume to be loaded only if an electrode at the loading site is activated. However, organic solvents (contact angle  $<90^\circ$ ) will spontaneously enter and flood the whole chip upon reaching the entrance [57] unless some kind of retracting force is applied. By orienting the needle vertically, the retracting force is supplied by the gravitational force on the liquid column within the needle. A potentially disposable multi-reagent loading interface was developed that could be integrated with upstream and downstream steps of the radiosynthesis process including [ $^{18}\text{F}$ ]fluoride concentration and purification [58].

## Concentration and loading of [<sup>18</sup>F]fluoride

Since cyclotrons can produce up to several Ci of [<sup>18</sup>F]fluoride in milliliter volumes of [<sup>18</sup>O]water, it is possible to directly load as much as tens of mCi of activity into the chip (maximum capacity of 17  $\mu$ L) without special measures. However, one typically does not want to produce such large quantities of [<sup>18</sup>F]fluoride and waste the majority after loading only a small amount into the chip.

Instead, larger amounts of radioactivity can be loaded by first concentrating the [<sup>18</sup>F]fluoride, using, for example, a quaternary methyl ammonium (QMA) cartridge. As typically done in macroscale synthesis, the desired amount of [<sup>18</sup>F]fluoride ion in [<sup>18</sup>O]water is passed through the cartridge, which traps the [<sup>18</sup>F]fluoride, and the [<sup>18</sup>O]water is collected for possible recycling. The cartridge is then washed and dried to remove residual water. By using a micro-cartridge, the trapped [<sup>18</sup>F]fluoride can be recovered with a very small volume of eluent. For example, Elizarov *et al.* concentrated 92% of 876 mCi of [<sup>18</sup>F]fluoride into a  $\sim$ 5 $\mu$ L volume [26], Lebedev *et al.* [30] and Bejot *et al.* [29] demonstrated release into 44  $\mu$ L volume, and we demonstrated release into  $\sim$ 12  $\mu$ L volume [59]. To improve compactness of the concentration process, one can integrate the resin directly into a microfluidic chip using techniques such as porous polymer monoliths, packed microfluidic channels, and resin-filled inserts [22, 60, 61]. Electrochemical trap and release methods may also be capable of [<sup>18</sup>F]fluoride concentration [62]. With such small output volumes, one can readily synthesize PET tracers in high radioactivity on the EWOD chip. Furthermore, in preliminary experiments, up to  $\sim$ 500 mCi [<sup>18</sup>F]fluoride solution has been concentrated, dispensed, and then dried on an EWOD microfluidic chip for use in a fluorination reaction [53], with no observable adverse impact on the chip or the reaction, suggesting that EWOD chips are compatible with high radioactivity levels.

Another strategy is to perform the [<sup>18</sup>F]fluoride concentration directly on chip. Using a chip where the bottom plate extends beyond the edge of the cover plate, a large (200  $\mu$ L) droplet of [<sup>18</sup>F]fluoride solution was loaded adjacent to the edge of the cover plate. The open droplet rapidly evaporated to a small size (5  $\mu$ L) that could be pulled into the chip for completion of the drying process and subsequent synthesis [33]. This new method may be helpful in high specific activity production as a recent report suggested that anion exchange resin can contribute additional fluorine-19 contamination into the reaction mixture [11].

## Liquid tracking and reaction monitoring

Using the existing electrodes in the EWOD chip, measurement of the electrical impedance of reagent and radioisotope droplets is possible. The impedance depends on many droplet characteristics, but measurements can be used to determine either droplet size, solute concentration, or type of solvent, provided the other two properties are known [63]. This capability could be used as a process monitoring mechanism to ensure the correct reagents have been loaded and transferred to the correct positions within the chip, or that the correct volumes have been loaded. High-sensitivity measurements of electrical properties such as the conductivity or permittivity are also possible [64, 65], potentially enabling monitoring of on-chip processes in real-time (e.g., determining the equivalence point when neutralizing a PET tracer during formulation, or neutralizing a radiometal solution prior to labeling).

## Product collection and purification

After synthesis, proof-of-concept efforts involved manual or automated collection of the crude product from the chip, followed by off-chip purification via solid-phase extraction (SPE) on miniature cartridges [31, 46] or injection into an analytical-scale HPLC system [48, 58]. These miniature purification systems are adequate due to the small masses of reagents used in microliter-scale syntheses, and chemical purity of our optimized methods for each tracer are comparable with conventional approaches and sufficient to meet regulatory requirements. Due to lower flow rates and narrower peak widths, analytical-scale HPLC purification typically results in 10–20x reduced sample volume compared with semi-preparative scale used in conventional macroscale synthesis. In addition, the separation time can often be reduced by using analytical-scale methods for purification. Other groups working on batch microreactors for radiochemistry have reported similar results [29, 30]. Similar improvements (reduced separation time and reduced final volume) may also be possible for miniature SPE methods with further development and optimization, though this remains to be demonstrated.

Because the use of external purification adds to the size and complexity of the overall system, on-chip methods have been pursued. Resnch *et al.* showed on-chip purification with custom resin-filled inserts in a disposable-cassette-based microfluidic system [22] and Tarn *et al.* developed a multi-stage solid-phase-extraction (SPE) chip suitable for use with continuous flow and dose-on-demand synthesis [66]. Initial proof-of-concept experiments on EWOD chips have shown that unreacted [ $^{18}\text{F}$ ]fluoride can be removed by incubating the crude product with an alumina surface [67]. This approach, however, requires a complex fabrication process and has limited [ $^{18}\text{F}$ ]fluoride trapping capacity; therefore, the use of alumina beads (diameter 80  $\mu\text{m}$ ) for trapping [ $^{18}\text{F}$ ]fluoride was also explored [68] (Figure 6). After incubation of the crude product with the beads, an on-chip filter comprising a line of polymer pillars (spacing 60  $\mu\text{m}$ ) was used to separate out the beads and leave a purified [ $^{18}\text{F}$ ]fallypride solution. Using this approach, a crude sample of [ $^{18}\text{F}$ ]fallypride (with ~84% purity) was increased to 99% purity. Because the particles containing the trapped [ $^{18}\text{F}$ ]fluoride and the droplet containing the purified product are spatially well-separated, one can accurately measure the amounts of radioactivity in the residual beads and the droplet using Cerenkov imaging [68], potentially providing a means for rapid *in situ* readout of the fluorination efficiency without having to remove the sample from the chip. Though only removal of [ $^{18}\text{F}$ ]fluoride was demonstrated so far, it may be possible to trap additional impurities from the crude product solution using beads of appropriate functionality, or by using on-chip SPE process where the desired product is trapped on a porous polymer monolith [69] or magnetic beads [70], and impurities are washed away.

## Outlook

Since the quantity of tracer needed in each production run is so miniscule (picomole to nanomole for  $^{18}\text{F}$ -labeled radiotracers), the synthesis of short-lived radiopharmaceuticals can benefit tremendously from being performed in tiny volumes. While manipulation of liquids at the microliter scale is extremely difficult with conventional radiochemistry automation approaches, it can be performed readily by digital microfluidic devices. At the microliter scale, the same amount of radioactivity can be used as in the macroscale, but

reagent consumption is dramatically reduced (100–1000x), even considering the higher concentrations sometimes needed, providing significant advantages for syntheses involving expensive precursors or biomolecules. In addition to production of radiotracers for PET, we expect that microvolume synthesis could also prove valuable for the preparation of radiotherapeutics and theranostic agents. An interesting concept for future exploration is whether, in all of these applications, the small volume could be leveraged as a means to economically enable a boost in concentration that may increase reaction rates and provide benefit for difficult radiosyntheses.

For the case of  $^{18}\text{F}$ -labeled PET tracers produced on chip, the small volumes also result in low fluorine-19 contamination and thus very high specific activities, even starting with minimal amounts of radioactivity. Similar benefits are expected when working with other isotopes for which the non-radioactive form may be present as an impurity in reagents, wetted materials, or the environment. It should be noted that improved SA occurs not only for conventional reactions such as nucleophilic fluorination, but also for isotopic exchange (IEX) reactions. When performed in macroscale systems, IEX reactions typically have very low SA due to the large excess of precursor needed, but reducing the precursor amount by 100–1000x by leveraging microliter reaction volumes increases the SA accordingly [71]. Microliter-scale synthesis may thus enable synthetic approaches to be used that have traditionally been limited by their difficulty to attain sufficient SA.

The lack of a complete automated platform for safe radiotracer production using EWOD digital microfluidics is currently a bottleneck in the wider use of EWOD microfluidics for radiosynthesis and in the routine use of higher radioactivities. Though automation of all the individual components of radiotracer production using EWOD digital microfluidics has been demonstrated, significant further efforts are needed as a next step to integrate the processes of radioisotope concentration, radiosynthesis, purification, and formulation, into an accessible and reliable prototype. The availability of a platform for experimentation with microscale radiochemistry will likely lead to increased diversity of synthesized tracers on EWOD and exploration of new microscale radiochemistry. An automated platform would also pave the way for use of the probes in humans, enabling development and optimization of scaled-up synthesis protocols, optimization of purification protocols, development of corresponding QC methods, and validation of the production process.

Because the physical size of the microfluidic chip size is so small, and many fluidic operations are controlled electronically, the entire tracer production system can be extremely small, requiring much less shielding than conventional systems, perhaps making it practical to make radiotracers on the benchtop. This could greatly reduce the upfront and operating costs associated with the development and production of radiotracers and enable affordable on-demand synthesis of diverse tracers. A commercial benchtop radiosynthesizer based on EWOD is currently being developed by Sofie Biosciences, Inc. in collaboration with our group. An important part of this effort is the development of a compact, low-cost, disposable cassette containing the chip, reagents, and all other elements (e.g. purification) needed to perform the synthesis, so that the end user need only swap cassettes (and software program) to produce different tracers. The realization of a bench-top production system will likely also require miniaturized, automated quality control testing. A comprehensive set of tests

would be necessary for human use of the tracers, while a smaller set of tests would be sufficient for preclinical use. Efforts are underway by several companies (e.g., QC-1, Traceability, ABT) to develop fully-automated QC testing systems for [ $^{18}\text{F}$ ]FDG and other tracers. Integration of QC testing into microfluidic chip-based platforms may provide even further advantages [72, 73]. An interesting prospect of performing synthesis in extremely tiny volumes is that reduced effort in purification or QC testing may be possible, especially if the total amount of reagent or solvent used is below the injectable limits set by regulatory agencies. This potential advantage warrants further investigation in order to streamline the overall tracer production process.

The development of automation will also address one of the current limitations of the EWOD platform, namely the relatively long synthesis times compared to other conventional and automated radiosynthesizers. Currently the reported synthesis times include unnecessary delays due to operations such as manually pipetting reagents to the chip, opening the chip and collecting crude product via pipette, and manually triggering various aspects of the software interface. With automation, reagent loading times and mixing times will be improved. In addition, slow temperature ramping times can be accelerated by improving the temperature control circuitry.

Another current limitation of the EWOD platform is the inability to perform intermediate purification steps that would enable multi-pot syntheses in addition to the one-pot syntheses that have been demonstrated to date. Performing such purifications on chip will likely be the preferred strategy in order to maintain the small volumes that are compatible with the volume capacity of the chip for downstream reactions and processes. Though on-chip removal of unreacted [ $^{18}\text{F}$ ]fluoride has been demonstrated, further development is needed to increase the range of impurities removed.

Finally, the open nature of the EWOD platform can result in unwanted solvent evaporation during high-temperature reactions. This generally requires the use of solvents with higher boiling points, such as DMSO, or a mixture of bulky alcohols and MeCN, to prevent the reaction droplet from completely drying out. While this restricts the range of solvents that can be used, it may not pose the same difficulties (i.e., removal) as when using DMSO in macroscale systems. The tiny volume of DMSO can be evaporated due to the high surface to volume ratio at the macroscale, or it can potentially be left in the reaction mixture. Residual amounts of DMSO were found not to interfere with reactions downstream of fluorination in [ $^{18}\text{F}$ ]FDG, [ $^{18}\text{F}$ ]FLT, and [ $^{18}\text{F}$ ]SFB syntheses, nor generate detectable impurities related to the presence of DMSO, but this may not be the case for all syntheses. Small amounts of residual DMSO may also not need to be removed in purification/formulation because dilution of the sample up to typical injection volumes will easily reduce the concentration of DMSO below allowed injection limits.

Despite these limitations, synthesis in microliter volumes offers unique opportunities such as achieving very high specific activities, reducing the consumption of precursors, operating at higher concentrations, and potentially simplifying purification procedures. Furthermore, the compact nature of the EWOD platform may enable the development of a compact, self-shielded synthesizer that could be used on a benchtop. A comprehensive comparison of

microliter-scale (EWOD) radiosynthesis to conventional and flow-through microfluidic approaches is include in Table 3.

## Acknowledgments

The authors gratefully acknowledge support for writing this review from the National Institute of Biomedical Imaging and Bioengineering (grant R21EB015540), the National Institute on Aging (grant R21AG049918), as well as Sofie Biosciences, Inc. and the National Institute of Mental Health (grant R44MH097271). We thank Melissa Moore, Maxim Sergeev, and Jeffrey Collins for valuable contributions to the manuscript.

## References

1. Mitra E, Quon A. Positron Emission Tomography/Computed Tomography: The Current Technology and Applications. *Radiologic Clinics of North America*. 2009; 47:147–160.10.1016/j.rcl.2008.10.005 [PubMed: 19195540]
2. Vallabhajosula S, Solnes L, Vallabhajosula B. A Broad Overview of Positron Emission Tomography Radiopharmaceuticals and Clinical Applications: What Is New? *Seminars in Nuclear Medicine*. 2011; 41:246–264.10.1053/j.semnuclmed.2011.02.003 [PubMed: 21624560]
3. Jones T, Rabiner EA. The development, past achievements, and future directions of brain PET. *J Cereb Blood Flow Metab*. 2012; 32:1426–1454.10.1038/jcbfm.2012.20 [PubMed: 22434067]
4. Matthews PM, Rabiner EA, Passchier J, Gunn RN. Positron emission tomography molecular imaging for drug development. *Br J Clin Pharmacol*. 2012; 73:175–186.10.1111/j.1365-2125.2011.04085.x [PubMed: 21838787]
5. Yaghoubi SS, Campbell DO, Radu CG, Czernin J. Positron Emission Tomography Reporter Genes and Reporter Probes: Gene and Cell Therapy Applications. *Theranostics*. 2012; 2:374–391.10.7150/thno.3677 [PubMed: 22509201]
6. Keng, PY.; Esterby, M.; van Dam, RM. Emerging Technologies for Decentralized Production of PET Tracers. In: Hsieh, C-H., editor. *Positron Emission Tomography – Current Clinical and Research Aspects*. 2012. p. 153-182. InTech
7. Anzellotti AI, McFarland AR, Ferguson D, Olson KF. Towards the Full Automation of QC Release Tests for [18F]fluoride-labeled Radiotracers. *Current Organic Chemistry*. 2013; 17:2153–2158.
8. Rensch C, Jackson A, Lindner S, et al. Microfluidics: A Groundbreaking Technology for PET Tracer Production? *Molecules*. 2013; 18:7930–7956.10.3390/molecules18077930 [PubMed: 23884128]
9. Miller PW, deMello AJ, Gee AD. Application of Microfluidics to the Ultra-Rapid Preparation of Fluorine-18 Labeled Compounds. *Current Radiopharmaceuticals*. 2010; 3:254–262.
10. Elizarov AM. Microreactors for radiopharmaceutical synthesis. *Lab Chip*. 2009; 9:1326–1333. [PubMed: 19417895]
11. Lu S, Giamis AM, Pike VW. Synthesis of [18F]fallypride in a micro-reactor: rapid optimization and multiple-production in small doses for micro-PET studies. *Curr Radiopharm*. 2009; 2:1–13.
12. Watts P, Pascali G, Salvadori PA. Positron Emission Tomography Radiosynthesis in Microreactors. *Journal of Flow Chemistry*. 2012; 2:37–42.10.1556/JFC-D-12-00010
13. Lebedev, A. Microfluidic devices for radio chemical synthesis In: *Microfluidic Devices for Biomedical Applications*. Elsevier; 2013. p. 594-633.
14. Pascali G, Watts P, Salvadori PA. Microfluidics in radiopharmaceutical chemistry. *Nuclear Medicine and Biology*. 10.1016/j.nucmedbio.2013.04.004
15. Rensch C, Waengler B, Yaroshenko A, et al. Microfluidic reactor geometries for radiolysis reduction in radiopharmaceuticals. *Appl Radiat Isot*. 2012; 70:1691–1697.10.1016/j.apradiso.2012.03.004 [PubMed: 22750198]
16. Brady F, Luthra S, Gillies J, Jeffery N. Use of microfabricated devices. 2005
17. Lu, SY.; Pike, VW. Micro-reactors for PET Tracer Labeling. In: Schubinger, P., editor. *PET Chemistry: The Driving Force in Molecular Imaging*. Springer; 2007. p. 271-287.



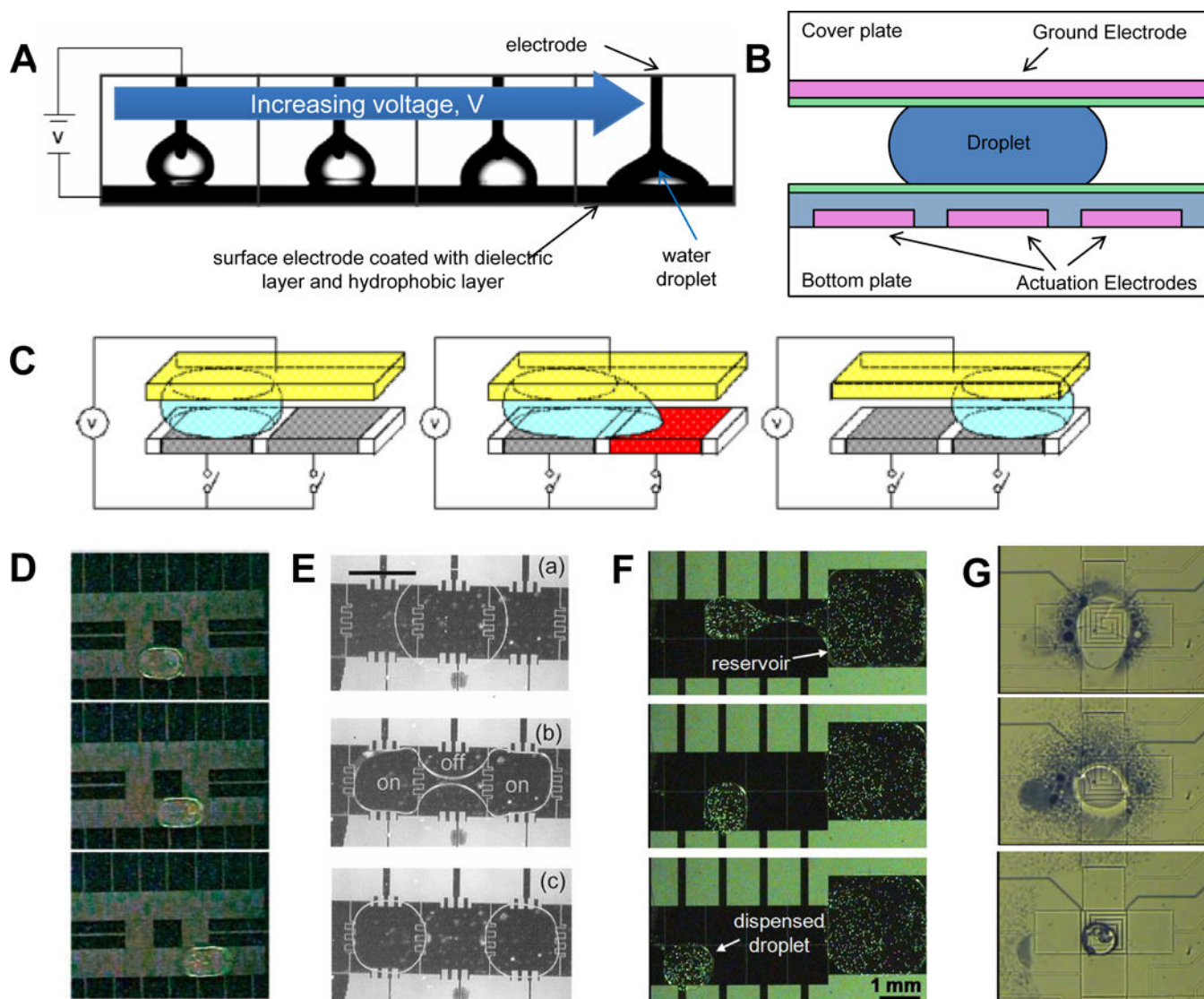
18. Gillies JM, Prenant C, Chimon GN, et al. Microfluidic technology for PET radiochemistry. *Applied Radiation and Isotopes*. 2006; 64:333–336.10.1016/j.apradiso.2005.08.009 [PubMed: 16290947]
19. Steel CJ, O'Brien AT, Luthra SK, Brady F. Automated PET radiosyntheses using microfluidic devices. *J Label Compd Radiopharm*. 2007; 50:308–311.10.1002/jlcr.1259
20. Zeng D, Desai AV, Ranganathan D, et al. Microfluidic radiolabeling of biomolecules with PET radiometals. *Nuclear Medicine and Biology*. 2013; 40:42–51.10.1016/j.nucmedbio.2012.08.012 [PubMed: 23078875]
21. Arima V, Pascali G, Lade O, et al. Radiochemistry on chip: towards dose-on-demand synthesis of PET radiopharmaceuticals. *Lab Chip*. 2013; 13:2328–2336.10.1039/C3LC00055A [PubMed: 23639996]
22. Rensch C, Lindner S, Salvamoser R, et al. A solvent resistant lab-on-chip platform for radiochemistry applications. *Lab Chip*. 2014; 14:2556–2564.10.1039/C4LC00076E [PubMed: 24879121]
23. Miller PW, Audrain H, Bender D, et al. Rapid Carbon-11 Radiolabelling for PET Using Microfluidics. *Chemistry – A European Journal*. 2011; 17:460–463.10.1002/chem.201002644
24. Liang SH, Yokell DL, Normandin MD, et al. First Human Use of a Radiopharmaceutical Prepared by Continuous-Flow Microfluidic Radiofluorination: Proof of Concept with the Tau Imaging Agent [18F]T807. *Mol Imaging*. 2014; 13:1–5.10.2310/7290.2014.00025
25. Lee C-C, Sui G, Elizarov A, et al. Multistep Synthesis of a Radiolabeled Imaging Probe Using Integrated Microfluidics. *Science*. 2005; 310:1793–1796.10.1126/science.1118919 [PubMed: 16357255]
26. Elizarov AM, van Dam RM, Shin YS, et al. Design and Optimization of Coin-Shaped Microreactor Chips for PET Radiopharmaceutical Synthesis. *J Nucl Med*. 2010; 51:282–287.10.2967/jnumed.109.065946 [PubMed: 20124050]
27. Tseng, W-Y.; Cho, JS.; Ma, X., et al. Toward reliable synthesis of radiotracers for positron emission tomography in PDMS microfluidic chips: Study and optimization of the [18F] fluoride drying process. *Technical Proceedings of the 2010 NSTI Nanotechnology Conference and Trade Show; Anaheim, CA*. 2010. p. 472-475.
28. Liu K, Lepin EJ, Wang M-W, et al. Microfluidic-based 18F-Labeling of Biomolecules for Immuno-Positron Emission Tomography. *Mol Imag*. 2011; 10:168–176.
29. Bejot R, Elizarov AM, Ball E, et al. Batch-mode microfluidic radiosynthesis of N-succinimidyl-4-[18F]fluorobenzoate for protein labelling. *J Label Compd Radiopharm*. 2011; 54:117–122.10.1002/jlcr.1826
30. Lebedev A, Miraghaie R, Kotta K, et al. Batch-reactor microfluidic device: first human use of a microfluidically produced PET radiotracer. *Lab Chip*. 2012; 13:136–145.10.1039/C2LC40853H [PubMed: 23135409]
31. Keng PY, Chen S, Ding H, et al. Micro-chemical synthesis of molecular probes on an electronic microfluidic device. *PNAS*. 2012; 109:690–695.10.1073/pnas.1117566109 [PubMed: 22210110]
32. Reichert DE. A Digital Revolution in Radiosynthesis. *J Nucl Med*. 2014; 55:181–182.10.2967/jnumed.113.132498 [PubMed: 24365652]
33. Chen S, Javed MR, Kim H-K, et al. Radiolabelling diverse positron emission tomography (PET) tracers using a single digital microfluidic reactor chip. *Lab Chip*. 2014; 14:902–910.10.1039/C3LC51195B [PubMed: 24352530]
34. Cho SK, Moon H, Kim C-J. Creating, transporting, cutting, and merging liquid droplets by electrowetting-based actuation for digital microfluidic circuits. *J MEMS*. 2003; 12:70–80.10.1109/JMEMS.2002.807467
35. Fiel SA, Yang H, Schaffer P, et al. Magnetic Droplet Microfluidics as a Platform for the Concentration of [18F]Fluoride and Radiosynthesis of Sulfonyl [18F]Fluoride. *ACS Appl Mater Interfaces*. 2015; 7:12923–12929.10.1021/acsami.5b02631 [PubMed: 26000709]
36. Fair R. Digital microfluidics: is a true lab-on-a-chip possible? *Microfluidics and Nanofluidics*. 2007; 3:245–281.10.1007/s10404-007-0161-8



37. Lee J, Moon H, Fowler J, et al. Electrowetting and electrowetting-on-dielectric for microscale liquid handling. *Sensors and Actuators A: Physical*. 2002; 95:259–268.10.1016/S0924-4247(01)00734-8
38. Pollack MG, Fair RB, Shenderov AD. Electrowetting-based actuation of liquid droplets for microfluidic applications. *Appl Phys Lett*. 2000; 77:1725–1726.10.1063/1.1308534
39. Chatterjee D, Hetayothin B, Wheeler AR, et al. Droplet-based microfluidics with nonaqueous solvents and solutions. *Lab Chip*. 2006; 6:199–206. [PubMed: 16450028]
40. Fan S-K, Hsieh T-H, Lin D-Y. General digital microfluidic platform manipulating dielectric and conductive droplets by dielectrophoresis and electrowetting. *Lab Chip*. 2009; 9:1236–1242. [PubMed: 19370242]
41. Zhao Y, Cho SK. Micro air bubble manipulation by electrowetting on dielectric (EWOD): transporting, splitting, merging and eliminating of bubbles. *Lab Chip*. 2007; 7:273–280.10.1039/B616845K [PubMed: 17268631]
42. Sista RS, Eckhardt AE, Srinivasan V, et al. Heterogeneous immunoassays using magnetic beads on a digital microfluidic platform. *Lab Chip*. 2008; 8:2188–2196.10.1039/B807855F [PubMed: 19023486]
43. Cho JS, Taschereau R, Olma S, et al. Cerenkov radiation imaging as a method for quantitative measurements of beta particles in a microfluidic chip. *Physics in Medicine and Biology*. 2009; 54:6757–6771. [PubMed: 19847018]
44. Dooraghi AA, Keng PY, Chen S, et al. Optimization of microfluidic PET tracer synthesis with Cerenkov imaging. *Analyst*. 2013; 138:5654–5664.10.1039/C3AN01113E [PubMed: 23928799]
45. Koag MC, Kim H-K, Kim AS. Efficient microscale synthesis of [18F]-2-fluoro-2-deoxy-d-glucose. *Chemical Engineering Journal*. 2014; 258:62–68.10.1016/j.cej.2014.07.077
46. Javed MR, Chen S, Kim H-K, et al. Efficient Radiosynthesis of 3'-Deoxy-3'-18F-Fluorothymidine Using Electrowetting-on-Dielectric Digital Microfluidic Chip. *J Nucl Med*. 2014; 55:321–328.10.2967/jnumed.113.121053 [PubMed: 24365651]
47. Koag MC, Kim H-K, Kim AS. Fast and efficient microscale radiosynthesis of 3'-deoxy-3'-[18F]fluorothymidine. *Journal of Fluorine Chemistry*. 2014; 166:104–109.10.1016/j.jfluchem.2014.07.033
48. Javed MR, Chen S, Lei J, et al. High yield and high specific activity synthesis of [18F]fallypride in a batch microfluidic reactor for micro-PET imaging. *Chem Commun*. 2014; 50:1192–1194.10.1039/C3CC47616B
49. Kim H-K, Javed MR, Chen S, et al. On-demand radiosynthesis of N-succinimidyl-4-[18F]fluorobenzoate on the electowetting-on-dielectric microfluidic chip for [18F]-labeling of protein. In progress.
50. Lapi SE, Welch MJ. A historical perspective on the specific activity of radiopharmaceuticals: What have we learned in the 35 years of the ISRC? *Nuclear Medicine and Biology*. 2013; 40:314–320.10.1016/j.nucmedbio.2012.12.010 [PubMed: 23357081]
51. Berridge MS, Apana SM, Hersh JM. Teflon radiolysis as the major source of carrier in fluorine-18. *Journal of Labelled Compounds and Radiopharmaceuticals*. 2009; 52:543–548.10.1002/jlcr.1672
52. Kung M-P, Kung HF. Mass effect of injected dose in small rodent imaging by SPECT and PET. *Nuclear Medicine and Biology*. 2005; 32:673–678.10.1016/j.nucmedbio.2005.04.002 [PubMed: 16243641]
53. Lazari, M.; Sergeev, M.; Liu, Z., et al. Study of specific activity in isotopic exchange radiofluorination performed on a microfluidic device. *World Molecular Imaging Congress*; 2014.
54. Shah GJ, Tata U, van Dam RM. Automation and interfaces for chemistry and biochemistry in digital microfluidics. *Technology*. 2014; 02:83–100.10.1142/S2339547814300030
55. Ding H, Sadeghi S, Shah GJ, et al. Accurate dispensing of volatile reagents on demand for chemical reactions in EWOD chips. *Lab on a Chip*. 2012; 12:3331–3340.10.1039/c2lc40244k [PubMed: 22825699]
56. Shah GJ, Ding H, Sadeghi S, et al. On-demand droplet loading for automated organic chemistry on digital microfluidics. *Lab Chip*. 2013; 13:2785–2795.10.1039/C3LC41363B [PubMed: 23670035]
57. Shah, GJ.; Ding, H.; Sadeghi, S., et al. Milliliter-to-microliter platform for on-demand loading of aqueous and non-aqueous droplets to digital microfluidics. *Proceedings of the 16th International*

- Solid-State Sensors, Actuators and Microsystems Conference (TRANSDUCERS); IEEE; 2011. p. 1260-1263.
58. Shah, GJ.; Lei, J.; Chen, S., et al. Automated injection from EWOD digital microfluidic chip into HPLC purification system. Proceedings of the 16th International Conference on Miniaturized Systems for Chemistry and Life Sciences; Royal Society of Chemistry, Okinawa, Japan. 2012. p. 356-358.
59. Lazari M, Narayanam MK, Murphy JM, Van Dam MR. Automated concentration of 18F-fluoride into microliter volumes. 2015
60. Ismail R, Iribarren J, Javed MR, et al. Cationic imidazolium polymer monoliths for efficient solvent exchange, activation and fluorination on a continuous flow system. RSC Advances. 2014; 4:25348–25356.10.1039/c4ra04064c
61. De Leonardis F, Pascali G, Salvadori PA, et al. On-chip pre-concentration and complexation of [18F]fluoride ions via regenerable anion exchange particles for radiochemical synthesis of Positron Emission Tomography tracers. Journal of Chromatography A. 2011; 1218:4714–4719.10.16/j.chroma.2011.05.062 [PubMed: 21683956]
62. Saiki H, Iwata R, Nakanishi H, et al. Electrochemical concentration of no-carrier-added [18F]fluoride from [18O]water in a disposable microfluidic cell for radiosynthesis of 18F-labeled radiopharmaceuticals. Applied Radiation and Isotopes. 2010; 68:1703–1708.10.1016/j.apradiso.2010.02.005 [PubMed: 20189817]
63. Sadeghi S, Ding H, Shah GJ, et al. On Chip Droplet Characterization: A Practical, High-Sensitivity Measurement of Droplet Impedance in Digital Microfluidics. Anal Chem. 2012; 84:1915–1923.10.1021/ac202715f [PubMed: 22248060]
64. Ma, X.; Chen, S.; Kim, C-JC.; van Dam, RM. Towards on-chip chemical reaction monitoring by EWOD impedance measurement. Proceedings of the 27th IEEE International Conference on Micro Electro Mechanical Systems (MEMS); San Francisco, CA. 2014. p. 338-341.
65. Ma, X. Ph.D. University of California; Los Angeles: 2014. Expanding the Capabilities of Microfluidic Systems for Positron Emission Tomography (PET) Tracer Synthesis and Analysis.
66. Tarn MD, Pascali G, De Leonardis F, et al. Purification of 2-[18F]fluoro-2-deoxy-d-glucose by on-chip solid-phase extraction. J Chromatogr A. 2013; 1280:117–121.10.1016/j.chroma.2013.01.032 [PubMed: 23375767]
67. Chen, S.; Lei, J.; van Dam, RM., et al. Planar alumina purification of 18F-labeled radiotracer synthesis on EWOD chip for positron emission tomography (PET). Proceedings of the 16th International Conference on Miniaturized Systems for Chemistry and Life Sciences; Okinawa, Japan. 2012. p. 1771-1773.
68. Chen, S.; Dooraghi, A.; Lazari, M., et al. On-chip product purification for complete microfluidic radiotracer synthesis. Proceedings of the 27th IEEE International Conference on Micro Electro Mechanical Systems (MEMS); San Francisco, CA. 2014. p. 284-287.
69. Yang H, Mudrik JM, Jebrail MJ, Wheeler AR. A Digital Microfluidic Method for in Situ Formation of Porous Polymer Monoliths with Application to Solid-Phase Extraction. Analytical Chemistry. 2011; 83:3824–3830.10.1021/ac2002388 [PubMed: 21524096]
70. Choi K, Ng AHC, Fobel R, et al. Automated Digital Microfluidic Platform for Magnetic-Particle-Based Immunoassays with Optimization by Design of Experiments. Anal Chem. 2013; 85:9638–9646.10.1021/ac401847x [PubMed: 23978190]
71. Liu Z, Li Y, Lozada J, et al. Stoichiometric Leverage: Rapid 18F-Aryltrifluoroborate Radiosynthesis at High Specific Activity for Click Conjugation. Angewandte Chemie International Edition n/a–n/a. 201310.1002/anie.201208551
72. Cheung, Shilin; Ly, Jimmy; Dam, R Michael. Capillary electrophoresis separation of 18F-labeled PET tracers from impurities: towards miniaturized quality control. Journal of Labelled Compounds and Radiopharmaceuticals. 2013; 56:S458.
73. Tarn, MD.; Isu, A.; Archibald, SJ.; Pamme, N. On-chip absorbance spectroscopy for the determination of optical clarity and pH for the quality control testing of [18F]FDG radiotracer. Proceedings of the 18th International Conference on Miniaturized Systems for Chemistry and Life Sciences; San Antonio, TX. 2014. p. 1077-1079.

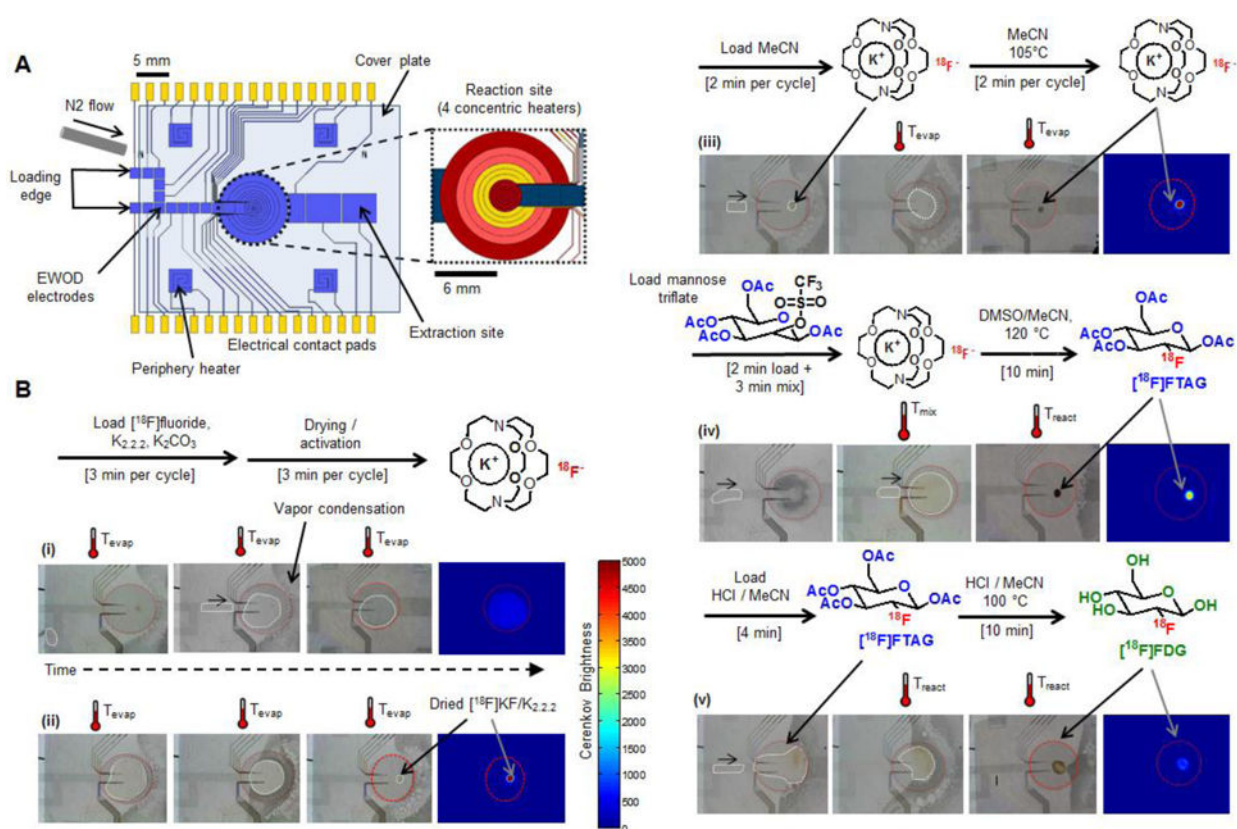
74. Lazari M, Collins J, Shen B, et al. Fully Automated Production of Diverse <sup>18</sup>F-Labeled PET Tracers on the ELIXYS Multireactor Radiosynthesizer Without Hardware Modification. *J Nucl Med Technol.* 2014; 42:203–210.10.2967/jnmt.114.140392 [PubMed: 25033883]
75. Long JZ, Jacobson MS, Hung JC. Comparison of FASTlab <sup>18</sup>F-FDG Production Using Phosphate and Citrate Buffer Cassettes. *J Nucl Med Technol.* 2013; 41:32–34.10.2967/jnmt.112.112649 [PubMed: 23318199]
76. Lee SJ, Oh SJ, Chi DY, et al. Simple and highly efficient synthesis of 3'-deoxy-3'-[<sup>18</sup>F]fluorothymidine using nucleophilic fluorination catalyzed by protic solvent. *Eur J Nucl Med Mol Imaging.* 2007; 34:1406–1409.10.1007/s00259-007-0391-8 [PubMed: 17384949]
77. Gomzina NA, Vasil'ev DA, Krasikova RN. Optimization of Automated Synthesis of 2-[<sup>18</sup>F]-Fluoro-2-deoxy-D-glucose Involving Base Hydrolysis. *Radiochemistry.* 2002; 44:403–409.
78. Seok Moon B, Hyung Park J, Jin Lee H, et al. Highly efficient production of [<sup>18</sup>F]fallypride using small amounts of base concentration. *Applied Radiation and Isotopes.* 2010; 68:2279–2284.10.1016/j.apradiso.2010.06.016 [PubMed: 20609592]
79. Tang G, Zeng W, Yu M, Kabalka G. Facile synthesis of N-succinimidyl 4-[<sup>18</sup>F]fluorobenzoate ([<sup>18</sup>F]SFB) for protein labeling. *Journal of Labelled Compounds and Radiopharmaceuticals.* 2008; 51:68–71.10.1002/jlcr.1481
80. Wheeler AR, Moon H, Kim C-J, et al. Electrowetting-Based Microfluidics for Analysis of Peptides and Proteins by Matrix-Assisted Laser Desorption/Ionization Mass Spectrometry. *Analytical Chemistry.* 2004; 76:4833–4838.10.1021/ac0498112 [PubMed: 15307795]
81. Barbulovic-Nad I, Yang H, Park P, Wheeler A. Digital microfluidics for cell-based assays. *Lab on a Chip.* 2008; 8:519. [PubMed: 18369505]



**Figure 1.**

Structure and operation of EWOD microfluidic chips. (A) Electronic control of the droplet interaction with the surface. (B) In a typical EWOD device, the droplet is sandwiched between two plates with the electrode configuration as shown. (C) By applying a voltage to one end of the droplet with an actuation electrode, a force is generated, pulling the droplet toward the activated electrode. (Diagram courtesy of Robin Garrell). This force enables several operations, including: (D) transport of droplets along a predetermined path, (E) droplet splitting, and (F) droplet dispensing from an on-chip reservoir. (G) By incorporating specialized heating electrodes, operations such as solvent evaporation are possible. D is reproduced with permission from reference [80] (Copyright © 2004 American Chemical Society); E is adapted with permission from reference [34] (Copyright © 2003 IEEE); F is reproduced from reference [81] with permission of The Royal Society of Chemistry.





**Figure 2.**

(A) Schematic of electrode pattern of EWOD chip for chemical synthesis. The central reaction zone has a volume capacity of  $\sim 17 \mu\text{L}$ . Inset shows magnified area of the heater with four concentric individually-controlled resistive heaters. (B) Sequence of optical micrograph images (grey background) of the EWOD chip with the corresponding Cerenkov images (blue background) at various times during the multistep radiosynthesis of  $[^{18}\text{F}]\text{FDG}$ . The central heating region is outlined in red, and the liquid droplets are outlined in white. Black arrows show the direction of droplet movement, and the activation of the heater is indicated by the thermometer symbol with adjacent temperature. Duration of each step is shown below the step. (i) Droplets containing  $[^{18}\text{F}]\text{fluoride}$  and phase-transfer catalyst are loaded and moved to the reaction site. The heater is activated to begin evaporation of solvent. (ii) Heat is applied until the solvent is fully evaporated, leaving a dried  $[^{18}\text{F}]\text{KF}/\text{K}_{2.2.2}$  residue. This cycle can be repeated to increase the amount of radioactivity loaded. (iii) Additional MeCN droplets are added and merged with the dried residue and then evaporated to remove residual water via azeotropic distillation. (iv) A droplet of precursor (mannose triflate) is loaded and mixed with the dried residue by heating at moderate temperature, followed by fluorination reaction at higher temperature. (v) Droplets containing a mixture of HCl/MeCN are added to the crude intermediate followed by hydrolysis at elevated temperature to form  $[^{18}\text{F}]\text{FDG}$ . After synthesis, the chip is opened and water is added to extract the crude product [5 min], and the crude product is purified via a miniature SPE cartridge [12 min]. Cerenkov images can be used to quantify the amount and distribution of

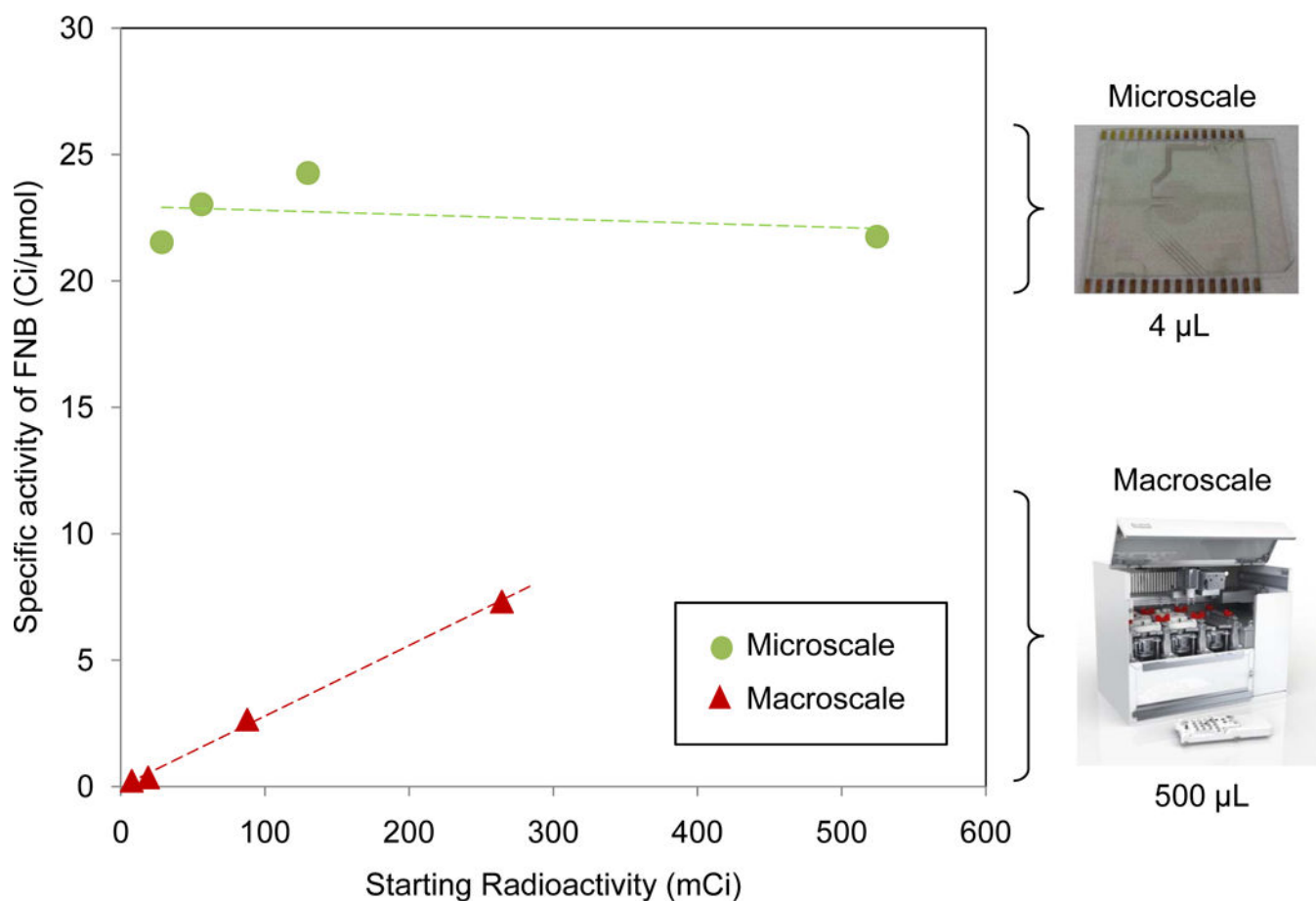
radioactivity on the chip after each step. Adapted with permission from reference [31] © 2012 by the National Academy of Sciences of the United States of America.

Author Manuscript

Author Manuscript

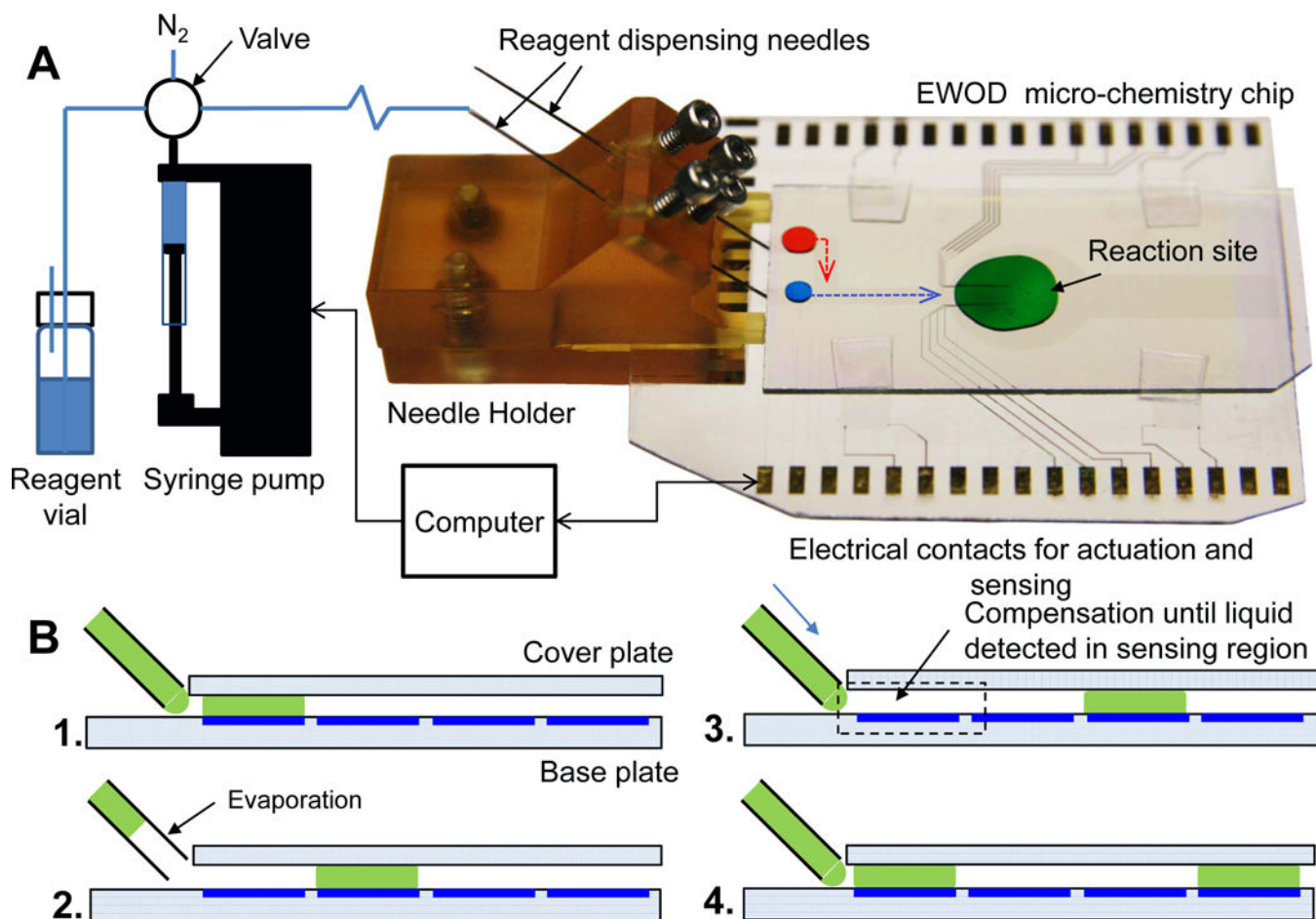
Author Manuscript

Author Manuscript

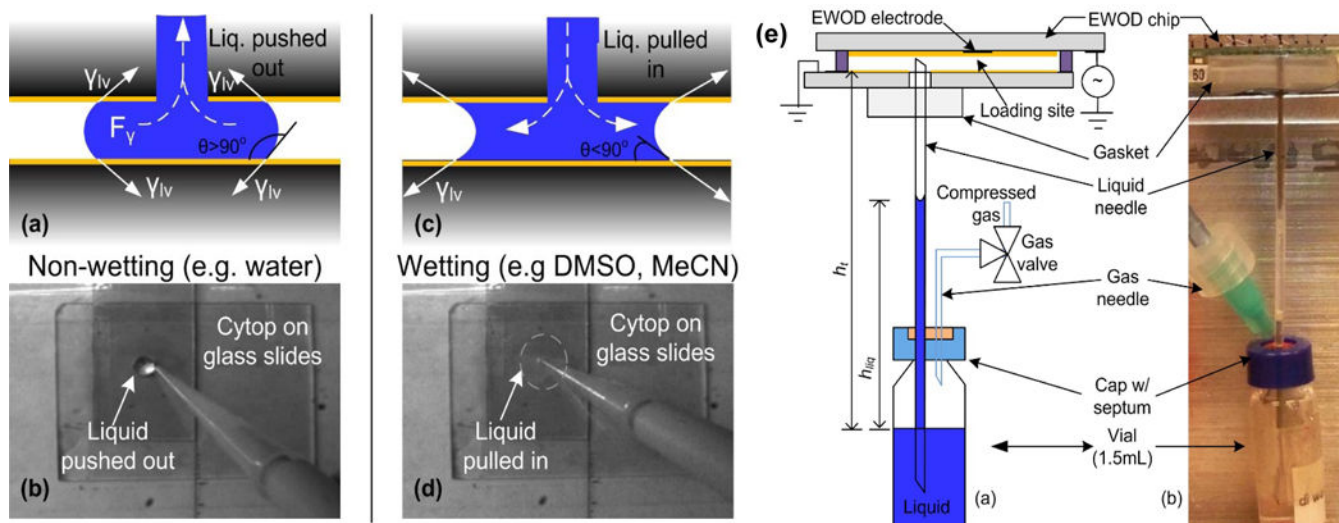


**Figure 3.** Comparison of specific activity (SA) of  $1\text{-}[^{18}\text{F}]\text{fluoro-4-nitrobenzene}$  ( $[^{18}\text{F}]\text{FNB}$ ) produced at the microscale versus the macroscale. At the microscale (green circles), SA is nearly constant, regardless of starting radioactivity; at the macroscale (red triangles), SA depends on starting radioactivity and high SA requires high starting radioactivity.



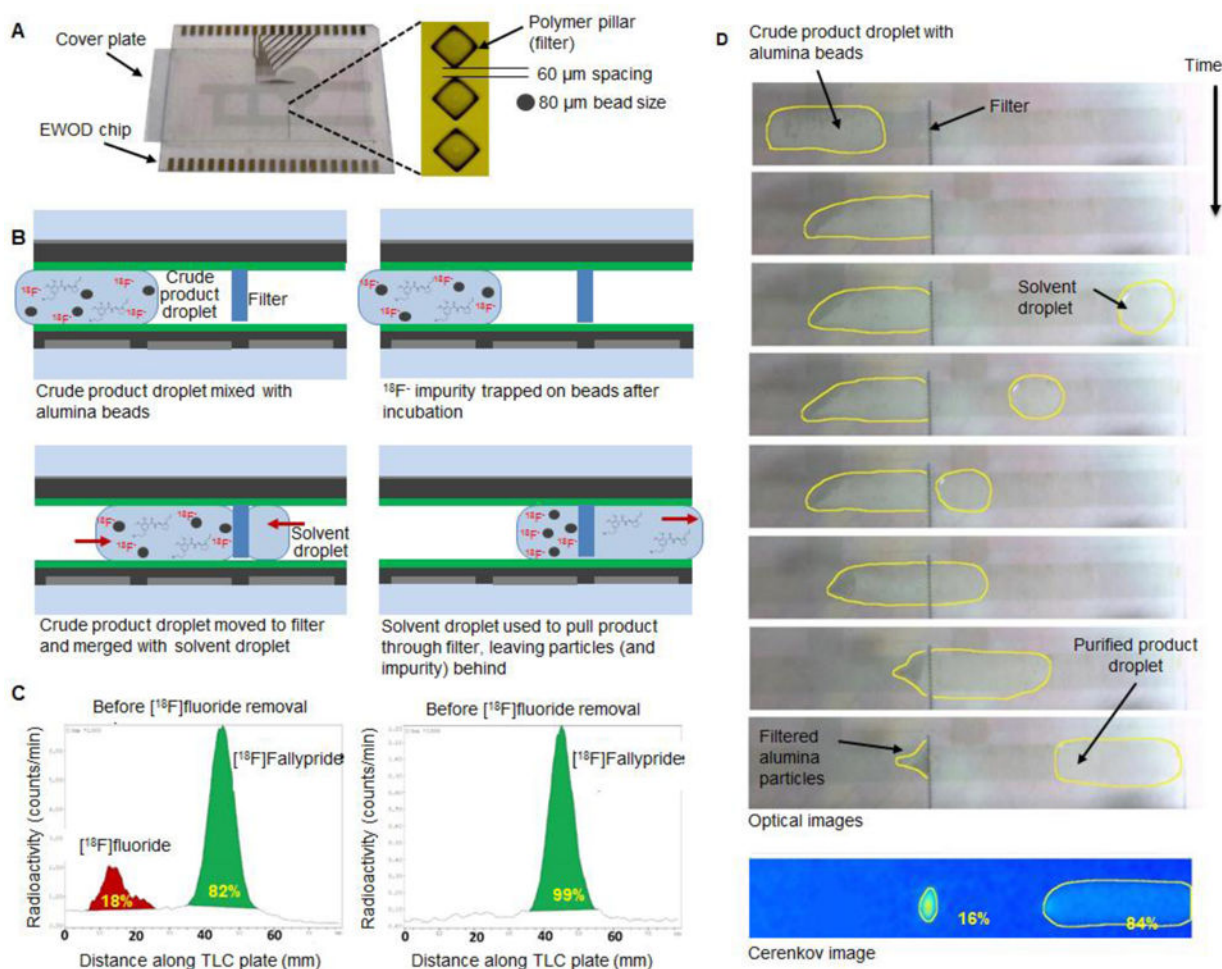


**Figure 4.** Automated dispensing of reagents to EWOD chip using a syringe pump. (A) Schematic of the fluid pathway and control system, including a photograph of the needle fixture and EWOD chip showing recently dispensed droplets. (B) Procedure for on-demand reagent delivery. After dispensing one droplet (step 1), undesired evaporation may occur at the tip of the dispensing needle (step 2). When the next droplet is needed, the control system advances the syringe pump until the liquid is detected electronically (step 3), and then dispenses the desired volume (step 4). Adapted from reference [55] with permission from The Royal Society of Chemistry.



**Figure 5.**


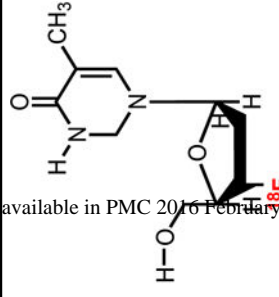
Automated dispensing of reagents in disposable format. For non-wetting liquids (a-b), the forward dispensing process controls the amount of reagent loaded; however, for wetting liquids (c-d), the reagent spontaneously enters the chip and must be controlled by a retracting force. (e) Schematic and photograph of a reagent loading mechanism relying on gas pressure to drive the reagent up to the chip, and gravitational force to retract excess liquid after loading. Adapted from reference [56] with permission from The Royal Society of Chemistry.

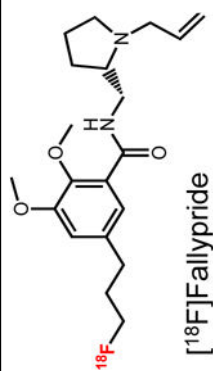
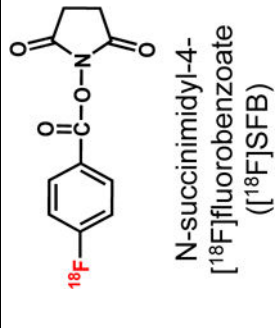


**Figure 6.** Partial on-chip purification for removal of  $^{18}\text{F}$ fluoride. (A) Photograph of modified EWOD chip for bead-based purification. (B) Schematic of on-chip purification process. The crude product droplet was mixed and incubated with alumina beads to trap unreacted  $^{18}\text{F}$ fluoride on the beads. The beads were then separated from the liquid to yield the purified product. (C) Radio-TLCs showing radiochemical purity of a  $^{18}\text{F}$ Fallypride sample before and after on-chip purification. (D) Optical micrographs of bead-based separation process. At the bottom is a Cerenkov image showing the distribution of radioactivity between beads and liquid. Portions of image © 2014 IEEE. Adapted with permission from reference [68].

Table 1

Summary of synthesis performance for four different radiotracers produced using EWOD chips (or simplified chips), and comparison to literature methods (macroscale and microscale). All efficiencies and yields are decay-corrected. N.R. means “not reported”. Note that synthesis times in EWOD include many manual processes and are expected to be reduced with automation. Adapted from reference [33] with permission from The Royal Society of Chemistry.

Tracer	Application	EWOD Methods				Literature Methods			Reference
		Crude RCY <sup>a</sup> (%)	RCY <sup>b</sup> (%)	Synthesis time <sup>c</sup> (min)	Full QC performed?	Reference	RCY (%)	Synthesis time <sup>c</sup> (min)	
 <sup>18</sup> F [18F]fluoro-2-deoxy-D-glucose ([18F]FDG)	Glucose metabolism	32 ± 15 (n=11) 45 ± 10 (n=2) 72 ± 13 (n=5) N.R.	22 ± 8 (n=11) 37 ± 13 (n=2) N.R. 71.2 ± ? (n=5)	75 50 ± 3 (n=2) + purif N.R. N.R. (shorter)	Yes No No No	[31] [33] [44] [45]	70 ± 9 (n=3) 83 ± 17 (n=40)	38 22	[74] [75]
 <sup>18</sup> F 3'-deoxy-3'-[18F]fluorodthymidine	DNA proliferation	74 ± 7 (n=6) 69 ± 8 (n=10) N.R.	56 ± 8 (n=6) 63 ± 5 (n=6) 71.3 ± ? (n=5)	40 ± 4 (n=6) + purif 63 N.R. (shorter)	No Yes No	[33] [46] [47]	69 ± 5 (n=5) 60 ± 5 (n=10)	65 71 ± 11	[74] [76]

Tracer	Application	EWOD Methods				Literature Methods		
		Crude RCY <sup>a</sup> (%)	RCY <sup>b</sup> (%)	Synthesis time <sup>c</sup> (min)	Full QC performed?	Reference	RCY (%)	Synthesis time <sup>e</sup> (min)
 <p><b>[<sup>18</sup>F]allylpride</b></p>	Neurotransmitter binding	84 ± 7 (n=6) 82 ± 6 (n=9) <sup>d</sup>	65 ± 11 (n=6) 65 ± 6 (n=7)	31 ± 1 (n=6) + purif 60	No Yes	[33] [48]	88 68 ± 2 (n=42)	50 <sup>e</sup> 51 ± 1 and van Dam
 <p><b>N-succinimidyl-4-<sup>18</sup>Ffluorobenzoate ([<sup>18</sup>F]SFB)</b></p>	Peptide or protein labeling	34 ± 10 (n=3)	19 ± 8 (n=5)	58 ± 5 (n=3) + purif	N/A	[33]	69 ± 8 (n=6) 64 ± 7 (n=?)	78 25–26

<sup>a</sup> Determined by multiplying purity of crude product (as determined by radio-TLC or radio-HPLC) by the radioactivity of the collected crude product (before purification), divided by the starting radioactivity.

<sup>b</sup> Radioactivity of the isolated product (after purification) divided by the amount of radioactivity that was loaded onto the chip.

<sup>c</sup> Synthesis time including purification. The notation “+ purif” is added when reported time does not include purification.

<sup>d</sup> Reported crude RCY is defined slightly differently in the paper than in this review and there was not sufficient data to convert it

<sup>e</sup> The reported synthesis time also includes formulation



Table 2

Summary of the fluorination efficiency (or decay-corrected crude RCY where indicated) as a function of various reaction parameters in the microdroplet radiosyntheses of [<sup>18</sup>F]FLT, [<sup>18</sup>F]fallypride, [<sup>18</sup>F]FDG, and [<sup>18</sup>F]SFB. The highlighted boxes represent the final conditions after all optimizations were performed. The optimized fluorination conditions were as follows: [<sup>18</sup>F]FLT (45 mM TBAHCO<sub>3</sub> and 90 mM precursor in 2 μL droplet for 3 min); [<sup>18</sup>F]fallypride (26 mM TBAHCO<sub>3</sub> and 77 mM precursor in 4 μL for 7 min); [<sup>18</sup>F]FDG (33 mM K<sub>2</sub>C<sub>2</sub>O<sub>4</sub>, 134 mM K<sub>2</sub>C<sub>2</sub>O<sub>4</sub>, and 104 mM precursor in 4 μL for 5 min); and [<sup>18</sup>F]SFB (108 mM K<sub>2</sub>C<sub>2</sub>O<sub>4</sub>, 195 mM K<sub>2</sub>C<sub>2</sub>O<sub>4</sub> and 87mM precursor in 2 μL for 4.5 min). “—” means not investigated.

[ <sup>18</sup> F]FLT Optimization	Fixed parameters	Reagent concentration 1x; Precursor:base ratio 2:1; Droplet size 4 μL		Reaction time (min)		Reaction time 1x; Precursor:base ratio 2:1; Droplet size 4 μL		Reaction time 3 min; Precursor:base ratio 2:1; Droplet size 4 μL		Reagent concentration 1x; Reaction time 5 min; Droplet size 4 μL		Reagent concentration 2x; Precursor:base ratio 2:1; Reaction time 3 min		
		3	5	7	10	1x	2x	5x	1:1	2:1	3:1	5:1	2	4
Varying parameters		3	5	7	10	1x	2x	5x	1:1	2:1	3:1	5:1	2	4
	Fluorination (%)	51±7% (n=3)	80±6% (n=10)	—	—	51±7% (n=3)	79±6% (n=2)	—	55±19 (n=3)	80±6% (n=10)	—	—	94±3% (n=9)	79±6% (n=2)
[ <sup>18</sup> F]fallypride Optimization	Fixed parameters	Reagent concentration 5x; Precursor:base ratio 5:1; Droplet size 4 μL		Reaction time 7 min; Precursor:base ratio 5:1; Droplet size 4 μL		Reagent concentration 5x; Reaction time 7 min; Droplet size 4 μL		Reagent concentration 5x; Reaction time 7 min; Droplet size 4 μL		Reagent concentration 5x; Reaction time 7 min; Droplet size 4 μL		Reagent concentration 5x; Precursor:base ratio 5:1; Reaction time 5 min		
		Varying parameters	3	5	7	10	1x	2x	5x	1:1	2:1	3:1	5:1	2
Fluorination (%)		—	54±18% (n=3)	73±7% (n=6)	—	27±11% (n=3)	44±11% (n=3)	73±7% (n=6)	—	—	51±4% (n=2)	73±7% (n=6)	29±30% (n=3)	54±18% (n=3)
	Fixed parameters	Reagent concentration 5x; Precursor:base ratio 3:1; Droplet size 4 μL		Reaction time 10 min; Precursor:base ratio 2:1; Droplet size 4 μL		Reagent concentration 5x; Reaction time 10 min; Droplet size 4 μL		Reagent concentration 5x; Reaction time 10 min; Droplet size 4 μL		Reagent concentration 5x; Reaction time 10 min; Droplet size 4 μL		Not investigated		
[ <sup>18</sup> F]FDG Optimization	Varying parameters	Reaction time (min)		Reaction time (min)		Reagent concentration <sup>a</sup>		Reagent concentration <sup>a</sup>		Reagent concentration <sup>a</sup>		Droplet size <sup>c</sup> (μL)		
		3	5	7	10	1x	2x	5x	1:1	2:1	3:1	5:1	2	4
Fluorination (%)		61±6% (n=3)	93±3% (n=2)	—	88±7% (n=11)	51±3% (n=4)	—	88±7% (n=11)	—	80±9% (n=4)	88±7% (n=11)	—	—	—
	Fixed parameters	Reagent concentration 4x; Precursor:base ratio 0.4:1; Droplet size 2 μL		Reaction time 4.5 min; Precursor:base ratio 0.4:1; Droplet size 2 μL		Reagent concentration <sup>a</sup>		Reagent concentration <sup>a</sup>		Reagent concentration <sup>a</sup>		Reaction time 4.5 min; Precursor:base ratio 0.4:1; Reagent Concentration 4x		
Varying parameters		3	4.5	7	10	1x	2x	5x	0.2:1	0.4:1	0.8:1	1.6:1	2	6
	Fluorination (%)	27±13% (n=6)	81±8% (n=4)	83±5% (n=4)	77±4% (n=3)	—	71±7% (n=7)	81±8% (n=4)	27±2% (n=2)	62±11% (n=3)	63±5% (n=3)	54±15% (n=2)	50±8% (n=5) (Crude RCY)	38±5% (n=4) (Crude RCY)

<sup>a</sup>Baseline (1X) concentrations were obtained from typical literature reports, for example: [<sup>18</sup>F]FLT [76], [<sup>18</sup>F]FDG [77], [<sup>18</sup>F]fallypride [78] and [<sup>18</sup>F]SFB [79]. Note that the extra volume of MeCN added at the beginning of fluorination is assumed to rapidly evaporate and thus its volume is not factored into the concentrations.

<sup>b</sup> Ratio was adjusted by fixing the base concentration and varying the precursor concentration. Note that for the [<sup>18</sup>F]SFB precursor:base optimization, the relative concentrations did not match a multiple of the baseline concentrations; instead, concentrations were [Precursor] = 7 mM; [K<sub>2</sub>CO<sub>3</sub>] = 9 mM and [K<sub>2</sub>.2.2] = 16 mM for the 0.4:1 ratio.

<sup>c</sup> Droplet size during fluorination reaction.



**Table 3**

Comparison of features of radiosynthesizer technologies.

Category of Comparison	Conventional synthesizers	Flow-through microfluidic synthesizers	Microliter-volume synthesizer (EWOD)
<b>Maturity of Technology</b>	Many commercial systems	Some commercial systems	No commercial systems yet
<b>Synthesis Diversity</b>	Some systems capable of multi-step syntheses with intermediate purification	Multi-step syntheses with no intermediate purification	Multi-step syntheses with no intermediate purification; diversity may increase with tech. advances
<b>Different tracers require plumbing reconfiguration?</b>	No (for cassette-based systems); Yes (for fixed-plumbing systems)	Yes	No
<b>Solvent Diversity</b>	Some systems limited to high-boiling solvents for high temperature reactions (to avoid exceeding pressure limits)	Unlimited	High-boiling solvents needed for high-temperature reactions (to reduce evaporation)
<b>Suitable for large scale production?</b>	Yes	Yes	Yes
<b>Suitable for high-throughput reaction optimization?</b>	No	Yes	Not yet demonstrated; possible in principle
<b>Number of production runs a day</b>	1 or multiple	Multiple (with system modifications)	Multiple
<b>Radiation shielding</b>	Hot cell / mini cell	Hot cell / mini cell	Self-shielded in principle (not yet demonstrated)
<b>Microscale components</b>	None	Reaction vessel only	Most of system (except HPLC purification)
<b>Typical reaction volume (<math>\mu\text{L}</math>)</b>	100–1000s	10–1000s (scales with radioactivity desired)	1–10
<b>Typical amount of reagent/precursor needed for production (nmol)</b>	10000s	100–10000s (depends on synthesis scale)	100s
<b>Enhancement in specific activity?</b>	None	Potential enhancement at low volumes	Yes
<b>Susceptible to clogging?</b>	Yes	Yes	No